Current Research in Food Science 5 (2022) 1668–1675

Contents lists available at ScienceDirect

Current Research in Food Science

journal homepage: www.sciencedirect.com/journal/current-research-in-food-science

Temperature of plasma-activated water and its effect on the thermal and chemical surface properties of cereal and tuber starches

Akua Y. Okyere [a], Prince G. Boakye [a], Eric Bertoft [b], George A. Annor [a,*]

[a] Department of Food Science and Nutrition, University of Minnesota, 1334 Eckles Avenue, Saint Paul, MN, 55108, USA
[b] Bertoft Solutions, Gamla Sampasvägen 18, 20960, Turku, Finland

ARTICLE INFO

Handling editor: Dr. Xing Chen

Keywords:
Plasma-activated water
Annealing
XPS analysis
Thermal properties
Hydration properties

ABSTRACT

High amylose and waxy starches from maize and potato were incubated with plasma-activated water (PAW) at 25 °C, 60 °C, and 80 °C temperatures to investigate PAW treatment effects on the starches' properties. At 60 °C incubation temperature, the starches were basically annealed with PAW. Annealing starches with PAW significantly increased ($p < 0.05$) the gelatinization parameters except for the enthalpy of gelatinization of waxy potato starch. Furthermore, starch swelling power significantly decreased while the water absorption capacity and solubility increased significantly when incubated at 80 °C. X-ray photoelectron spectroscopy (XPS) analysis showed the oxidation of C–C/C–H and C–O into carboxyl groups in waxy and high amylose maize starches incubated with PAW at 60 °C and 80 °C, respectively. In addition, cross-linking was observed in waxy maize and high amylose potato incubated with PAW at 80 °C and 25 °C, respectively. Overall, the results indicated PAW temperature is an important factor in modifying cereals and tuber starches with PAW.

1. Introduction

Native starches typically exist in granular form and comprise a linear molecule (amylose) and a highly branched molecule (amylopectin). The former consists of α-(1,4) glycosidic bonds with 1% α-(1,6) branched points, while the latter has α-(1,4) glycosidic bonds interconnected through 5% α-(1,6) linkages (Hizukuri et al., 1981, 1983; Pérez and Bertoft, 2010). Starches typically contain 20–35% amylose and 65–80% amylopectin. There are, however, high amylose and waxy starches with >35% amylose and <5% amylose, respectively (X. Wu et al., 2006). High amylose starch is inherently resistant to digestion (RS2). It forms strong, cohesive gels, while waxy starches have better paste clarity, form soft, sticky gels, and are inherently non-resistant to digestion (Li et al., 2019). Resistant starch type 2 (RS2) refers to raw starch granules, mostly B-type crystalline starches, resistant to enzyme digestion (Li et al., 2019).

Starch modification is necessary to improve starches' functionality, heat and shear tolerance during industrial processing (Laovachirasuwan et al., 2010). Furthermore, modified starches are used as fat replacers in yogurt, thickeners, stabilizers, gelling, and encapsulating agents (Bemiller, 1997). Physical modification techniques such as annealing and cold plasma technology have proven to be effective in altering the structure and functionality of starches and do not involve the generation of hazardous chemical waste (Tester and Debon, 2000; Thirumdas et al., 2017a; Zhu, 2017). Annealing is a hydrothermal treatment characterized by the treatment of starch in intermediate (40–55% w/w) or excess (>60% w/w) water contents above the glass transition temperature (Tg) but below the onset gelatinization temperature of starch (Hoover, 2010). Cold plasma is a partially ionized gas made of photons, free radicals, reactive oxygen, and nitrogen species. Cold plasma generation involves low or atmospheric pressure devices (Thirumdas et al., 2017a; Zhu, 2017). Cold plasma can be applied directly to materials during modification or as plasma-activated water (Okyere, Rajendran, et al., 2022). Plasma-activated water is a chemically reactive water obtained using atmospheric plasma devices to generate reactive species directly inside or above the water's surface over time. Reactive oxygen and nitrogen species such as atomic oxygen, hydroxyl radicals, ozone, hydrogen peroxide, nitric oxide, nitrates, nitrites, and peroxynitrites are generated in the gas-water interface when using air as the discharge gas (Lukes et al., 2014). The pH of plasma-activated water is low (acidic), while the oxidative-reductive potential and electrical conductivity are high due to the reactive species generated in the gas-water interface. Thus, PAW is suitable for hindering microbial growth, enhancing seed germination, and in our case, starch modification (Thirumdas et al.,

* Corresponding author.
E-mail addresses: okyer011@umn.edu (A.Y. Okyere), eric.bertoft@abo.fi (E. Bertoft), gannor@umn.edu (G.A. Annor).

https://doi.org/10.1016/j.crfs.2022.09.020
Received 11 May 2022; Received in revised form 23 August 2022; Accepted 16 September 2022
Available online 26 September 2022

2018).

Studies reported on the effect of PAW on starches are limited. Yan et al. (2020) utilized plasma-activated water and heat moisture treatment (PAW-HMT) to modify waxy and normal maize starches. They observed an increase in resistant starches and solubility and a decrease in swelling power of PAW-HMT modified starches. Aaliya et al. (2022) investigated the effect of annealing and heat-moisture treatment with PAW on talipot starch. The authors reported an increase in retrogradation and resistant starch content after treatment. However, the effect of PAW alone on high amylose and waxy potato starch remains to be explored. In addition, starch gelatinization using PAW has not been reported. Potato starches are high in phosphate groups and have unique properties making them useful for diverse industries (Whistler and Bemiller, 2009). Therefore, it is imperative to examine alternative ways to enhance its functionality and thermal properties. This study investigated the effects of PAW only, PAW and annealing, and PAW at 80 °C on high amylose and waxy potato starches. In addition, the study investigated the impact of PAW treatments on high amylose and waxy maize starches. The X-ray photoelectron spectroscopy, Fourier transform infrared spectroscopy with attenuated total reflectance, and differential scanning calorimetry were used to determine the effects of the treatments on the thermal and chemical surface properties of starches. This study is essential in expanding our knowledge on the effect of PAW treatments on starches' surface chemistry, thermal, and functional properties. Furthermore, we hypothesize that these treatments would significantly impact the characteristics of starches, and as such, can be an alternative means of starch modification.

2. Materials and methods

2.1. Materials

Waxy maize (AMIOCA) and potato (ELIANE 100) starches and high amylose maize (HYLON V) starch used for the experiment were obtained from Ingredion Incorporated (Bridgewater, NJ, USA). High amylose potato (44% amylose) was obtained from Andreas Blennow, Ph.D., Department of Plant and Environmental Sciences, University of Copenhagen, Denmark. The atmospheric pressure plasma jet (APPJ) (model: Dyne-A-Mite IT) operating at 120 V was obtained from Enercon Industries (Menomonee Falls, Wisconsin, USA). Chemicals used in this study were of analytical grade.

2.2. Plasma-activated water production and starch modification

2.2.1. Generating plasma-activated water

Deionized water (200 mL) was treated with an APPJ for 30 min with constant stirring. Air at 80 pound-force per square inch (psi) was used as the discharge gas. This was repeated to obtain 4 L of plasma-activated water. The distance between the APPJ probe and the surface of the water was 10 cm. The pH, oxidative-reductive potential (ORP), and conductivity were measured using the SURE TEST® pH/EC/TDS/mV LAB METER (Greentrees Hydroponics, California, USA). The measured parameters are presented in Table 1.

Table 1
pH, ORP, and electric conductivity of plasma-activated water.

Water	pH	Oxidative-Reductive Potential (ORP) (mV)	Conductivity (μS/cm)
DDW	6.5 ± 0.1[b]	345.5 ± 0.7[a]	1.7 ± 0.0[a]
PAW	2.6 ± 0.1[a]	581.0 ± 2.8[b]	749.0 ± 1.4[b]

DDW-Double Distilled Water, PAW-Plasma-Activated Water; Values are expressed as duplicate measurement of the mean ± standard deviation. The superscript on the means shows significant differences ($p < 0.05$) between the parameters measured for DDW and PAW.

2.2.2. Treatment of starches with plasma-activated water

Approximately 1.5 g of starch was mixed with plasma-activated water (100 mL) and incubated at 25 °C and 80 °C for 12 h. At 25 °C, we sought to investigate the effect of PAW only on starches, while at 80 °C, we determined the impact of gelatinizing starch in PAW on starches' properties.

Starches were annealed by mixing starch (1.5g) with plasma-activated water (100 mL) and incubated at 60 °C for 12 h.

The starch slurries were constantly shaken at 200 rpm during treatment. The slurries were then centrifuged at 2000 g (10 min), after which the supernatant was carefully discarded. Next, the pellets were washed with deionized water and centrifuged at 2000 g (10 min). Washing and centrifugation were repeated thrice, after which the remaining pellet was reconstituted in water, frozen and lyophilized. Finally, the treated starches were kept in snap cap vials in a desiccator until further analysis. Native starches were used as control.

2.3. Amylose content determination

Determination of the amylose content in the high amylose potato starch was done based on methods described by Chrastil (1987). Starch samples (10–20 mg) were suspended in 85% methanol and incubated at 60 °C for 30 min with occasional mixing to extract all lipids. The samples were centrifuged at 1500 rpm for 5 min after which the supernatant was discarded. The lipid extraction was repeated. Samples were solubilized for 30 min at 100 °C in 6 mL of urea-DMSO (0.6M urea in 90% DMSO). Subsequently, 0.1 mL of the solubilized sample was transferred into 5 mL of 0.5% trichloroacetic acid in a separate test tube. The solutions were mixed, after which 0.05 mL of 0.01N I_2-KI solution (1.27 g I_2/L + 3 g KI/L) was added and vortexed immediately and left to stand at 25 °C. The blue color formed was read at 620 nm after 30 min against water (blank). Hylon VII corn starch was used as our standard amylose sample.

The amylose content was determined based on the formula

$$Amylose\ content\ (\%) = \frac{A \times 45.8 \times 5.15 \times 60}{Sample\ weight \times 1000} \times \frac{100}{100 - moisture\ content} \quad (1)$$

where A is the absorbance of the sample.

2.4. Fourier transform infrared spectroscopy-attenuated total reflectance (FTIR-ATR) measurement

The FTIR-ATR measurements were done using a Nicolet iS50 FTIR (Thermo Fisher Scientific, MN, USA) equipped with a Deuterated Triglycine Sulfate Attenuated Total Reflection (DGTS ATR) detector by spreading a thin layer of starch onto the diamond crystal and applying pressure using the pressure tower. A total of 64 scans were recorded with a spectral resolution of 4 cm^{-1} within a spectral range of 4000 to 650 cm^{-1}. The spectra were collected using the OMNIC software. All the samples were recorded against a background spectrum (which is a spectrum without a starch sample in place). The spectra were baseline corrected and normalized using the Min/Max method (Pu et al., 2011), after which the intensities of the bands at 930 and 1150 cm^{-1} were computed using the OPUS 7.0 software (Bruker, Madison, WI, USA).

2.5. Thermal analysis

The Differential Scanning Calorimeter (DSC) from Mettler Toledo (Columbus, OH, USA) was used to measure the gelatinization onset, peak and conclusion temperature, as well as the enthalpy of gelatinization of the starches based on methods described by Okyere et al. (2019) with slight modifications. This was done by heating one part starch (4 mg) in three parts (12 mg) deionized water in a hermetically sealed DSC pan from 25 °C to 120 °C at a heating rate of 5 °C/min. Starches were equilibrated to room temperature for approximately 30

min prior to testing. The starches were then tested against an empty pan used as a reference. The results were analyzed using the STARe thermal analysis software version 11.00. Samples were run in duplicate.

2.6. X-ray photoelectron spectroscopy analysis

The chemical surface analysis measurements were performed on a PHI 5000 Versa Probe III XPS system (ULVAC-PHI) (Chanhassen, MN, USA) using a monochromatic Al K_α X-ray source (1486.6 eV). The base pressure was 3.0×10^{-8} Pa. Starch samples were mounted on a piece of sticking tape on the sample holder. The sample was not conductive, and the charge neutralization was applied during the data collection. The measurements were conducted using an X-ray spot size of 0.1×0.1 mm^2 with a power of 25 W under 15 kV. The survey spectra were measured using 280 eV pass energy and 1.0 eV/step. The high-resolution spectra were collected using 55 eV pass energy and 0.1 eV/step. The atomic percentages were calculated from the survey spectra using the Multipak software provided with the XPS system. For the high-resolution data, the lowest binding energy C_{1s} peak (C–C and C–H) was set at 285.0 eV and used as the reference. The curve fitting used a combination of Gaussian/Lorentzian function with the Gaussian percentages being 80% or higher (Bie et al., 2016).

2.7. Hydration properties of starch

2.7.1. Swelling power and solubility

The solubility and swelling power of the starch samples were determined using the method by X. Han et al. (2022), with some modifications. Blended suspensions with 5% starch samples were heated at 85 °C for 30 min and then centrifuged at 3000 *g* for 10 min. The precipitates were weighed, and the supernatants dried at 135 °C for 2 h. The solubility (%) and swelling power (g/g) were expressed using the following equations:

$$Solubility\ (\%) = \frac{A}{W} \times 100 \quad (2)$$

$$Swelling\ Power\ (g/g) = \frac{B}{W} \times (1 - S) \quad (3)$$

Where A is the residual starch mass of supernatant after drying; W is the weight of starch sample; B is the precipitate weight after centrifugation; S is the solubility of the sample. The experiments were run in duplicate.

2.7.2. Water absorption capacity

The water absorption capacity of the starch samples was determined using the method by X. Han et al. (2022), with some modifications. Approximately 6% starch solution was prepared with the samples and distilled water, and vortexed for 5 min to mix the solution well. The solutions were then placed at ambient temperature (~ 22 °C) for 30 min to allow sufficient absorption of water by the starch samples. Afterwards, the mixture was centrifuged at 3000 *g* for 10 min and the supernatant discarded. The precipitate was then weighed. The water absorption capacity was calculated using the following equation:

$$Water\ Absorption\ Capacity\ (\%) = \frac{M - W}{W} \times 100 \quad (4)$$

Where M is the weight of the precipitate; and W is the weight of the starch sample. The analysis was done in duplicate.

2.8. Statistical analysis

All results were statistically analyzed by one-way ANOVA with Statgraphics Centurion XVI, version 16.1.0 (Stat Point, Warrenton, VA, U.S.A.). Duncan's multiple range test was used to determine statistical significance between means at $p < 0.05$.

3. Results and discussion

3.1. Physicochemical properties of plasma-activated water

The pH, Oxidative-Reductive Potential (ORP), and electrical conductivity of Double Distilled Water (DDW) and PAW are presented in Table 1. The pH of DDW significantly decreased from 6.5 to 2.6 after 30 min of APPJ treatment. The use of air as the discharge gas in PAW generation results in the formation of reactive species such as hydroxyls ($OH^{\cdot}$), nitrate (NO_3^-), and nitrites (NO_2^-) at the gas-water interface (Lukes et al., 2014). These species continue to undergo several reactions resulting in the formation of hydrogen peroxide (H_2O_2), nitric acid (HNO_3), and peroxynitrous acid in PAW, which makes the water acidic (Oehmigen et al., 2010). The conductivity measures the flow of ions and electric currents in water (Thirumdas et al., 2018). We observed an increase ($p < 0.05$) in the conductivity from 1.7 in DDW to 749 μS/cm in PAW which could be attributed to the generation of reactive oxygen species (ROS) and reactive nitrogen species (RNS) in PAW (Lukes et al., 2014). The ORP of PAW also increased significantly after treatment from 345.5 to 581 mV. The formation of ROS such as H_2O_2, accounts for the increase observed in ORP (Lukes et al., 2012).

3.2. Thermal properties

Annealing of the starches with PAW significantly increased the

Table 2
Thermal properties of PAW treated and untreated starches.

Samples	T_o (°C)	T_p (°C)	T_c (°C)	T_c-T_o (°C)	ΔH J/g
WMS	65.1 ± 0.4[a]	70.1 ± 0.1[a]	76.5 ± 0.2[a]	11.4 ± 0.2[b]	5.3 ± 0.1[a]
PAW-WMS 25 °C	64.3 ± 0.4[a]	69.8 ± 0.3[a]	75.9 ± 0.3[a]	11.6 ± 0.1[b]	6.1 ± 0.1[b]
PAW-WMS 60 °C	70.3 ± 0.4[b]	73.3 ± 0.4[b]	77.9 ± 0.1[b]	7.7 ± 0.4[a]	7.8 ± 0.1[c]
HAMS	69.3 ± 0.1[a]	73.7 ± 0.4[a]	81.2 ± 0.1[a]	11.9 ± 0.3[a]	1.8 ± 0.1[a]
PAW-HAMS 25 °C	68.6 ± 0.0[a]	73.9 ± 0.3[a]	81.9 ± 0.3[a]	13.3 ± 0.3[b]	1.8 ± 0.0[a]
PAW-HAMS 60 °C	72.2 ± 0.4[b]	76.9 ± 0.1[b]	84.1 ± 0.4[b]	11.9 ± 0.0[a]	4.0 ± 0.0[b]
WPS	63.3 ± 0.0[a]	67.9 ± 0.0[a]	72.6 ± 0.0[a]	9.3 ± 0.0[b]	12.5 ± 0.0[b]
PAW-WPS 25 °C	63.2 ± 0.0[a]	67.8 ± 0.1[a]	72.6 ± 0.2[a]	9.4 ± 0.2[b]	11.9 ± 0.0[a]
PAW-WPS 60 °C	70.0 ± 0.4[b]	73.3 ± 0.4[b]	77.1 ± 0.3[b]	7.1 ± 0.1[a]	11.9 ± 0.2[a]
HAPS	66.7 ± 0.1[a]	70.7 ± 0.1[a]	75.1 ± 0.1[a]	8.3 ± 0.0[b]	10.4 ± 0.0[a]
PAW-HAPS 25 °C	67.3 ± 0.0[b]	71.4 ± 0.0[b]	76.3 ± 0.0[b]	9.0 ± 0.1[c]	11.0 ± 0.0[b]
PAW-HAPS 60 °C	74.8 ± 0.2[c]	77.3 ± 0.2[c]	80.8 ± 0.3[c]	6.0 ± 0.1[a]	13.7 ± 0.0[c]

[a] Values are expressed as duplicate measurement of the mean ± standard deviation. Means with different superscript letters shows significant differences ($p < 0.05$) between treated and untreated starches of the same type; The different incubation temperatures for the starches are attached to the sample name.
WMS: Waxy Maize Starch, PAW-WMS 25 °C: Plasma-Activated Water Waxy Maize Starch 25 °C, PAW-WMS 60 °C: Plasma-Activated Water Waxy Maize Starch 60 °C, HAMS: High Amylose Maize Starch, PAW-HAMS 25 °C: Plasma-Activated Water High Amylose Maize Starch 25 °C, PAW-HAMS 60 °C: Plasma-Activated Water High Amylose Maize Starch 60 °C, WPS: Waxy Potato Starch, PAW-WPS 25 °C: Plasma-Activated Water Waxy Potato Starch 25 °C, PAW-WPS 60 °C: Plasma-Activated Water Waxy Potato Starch 60 °C, HAPS: High Amylose Potato Starch, PAW-HAPS 25 °C: Plasma-Activated Water High Amylose Potato Starch 25 °C, PAW-HAPS 60 °C: Plasma-Activated Water High Amylose Potato Starch 60 °C.
T_o: onset temperature, T_p: peak temperature, T_c: conclusion temperature, ΔH: enthalpy of gelatinization, T_c-T_o: (conclusion temperature – onset temperature) Gelatinization temperature range.

gelatinization parameters (T_o, T_p, T_c, and ΔH) of the starches except for ΔH in waxy potato starch (PAW-WPS 60 °C) (Table 2). Treatment of the starch with PAW only, significantly increased the T_o (67.3 °C), T_p (71.4 °C), T_c (76.3 °C) and ΔH (11.0 J/g) in high amylose potato starch. Also, incubating waxy maize starch in PAW only (PAW-WMS 25 °C) increased ($p < 0.05$) the ΔH from 5.3 to 6.1 J/g. The higher gelatinization temperatures suggest that treating starches in PAW only (in the case of HAPS) or annealing starches with PAW resulted in the reorganization of the double helices into a perfect crystalline structure (Vamadevan et al., 2013). In addition, plasma-activated water is rich in H^+ ions which could induce the formation of additional hydrogen bonds between the double helices due to the close alignment of the strands and strengthen the crystal structure (Bogracheva et al., 2001). This alignment hinders plasticization during heating and increases the gelatinization temperatures (Vamadevan et al., 2013).

The increases observed in ΔH indicate the presence of longer double helices formed by the organization of the unraveled ends of the external chains of the amylopectin (Qi et al., 2003). In the case of WPS treated with PAW only, and annealed with PAW, the reactive species in PAW possibly distorted the crystal structure and decreased the ΔH (Noda et al., 2009). The temperature ranges (T_c-T_o) increased ($p < 0.05$) in the high amylose starches treated with PAW only and decreased ($p < 0.05$) in all starches annealed with PAW, except for PAW-HAMS, in which it remained the same. The lower melting temperature ranges of the starches annealed with PAW suggest that annealing of starches with PAW leads to the formation of homogenous amylopectin crystals that are more stable (Tester and Debon, 2000; Ratnayake et al., 2001; Annor et al., 2014b). However, when the incubation temperature goes beyond the gelatinization temperatures of the starches, they become amorphous, as in the case of the PAW starches incubated at 80 °C. We did not report on these gelatinization parameters since they were amorphized (Figure S1). Overall, the melting temperatures of the high amylose starches were higher than their respective waxy starches. This is because the gelatinization temperatures increase with increasing amylose content (Matveev et al., 2001).

3.3. Swelling power and solubility

When compared to the control starches, a significant reduction in the swelling power (SP) of the starches was observed when treated with PAW irrespective of the temperature except for high amylose maize (Fig. 1). Within the PAW treatments, the SP of the HAMS and WPS treated with PAW only and annealed with PAW were statistically similar but decreased ($p < 0.05$) at 80 °C. In the case of WMS, reductions in SP were observed even at 60 °C. HAPS was unique in the sense that increases in SP was observed after annealing with PAW and at 80 °C and it is unclear why this was observed. The reductions observed in the swelling power suggest that the reactive species present in PAW induced the oxidation of lipids in the high amylose maize starch (Sarangapani et al., 2017). Thus, these lipids could form complexes with the starches, which would inhibit the swelling ability of the starches (Tester and Morrison, 1990; Eliasson and Ljunger, 1988). In the case of the other starches, PAW could induce the acid hydrolysis of the amorphous and crystalline structures decreasing their ability to bind water and swell (Yan et al., 2020).

The solubility of waxy maize and waxy potato starches treated with PAW only (7.2%, 22.8%) and annealed with PAW (42.0%, 29.1%) was significantly higher than their control starches (Fig. 2). PAW-WMS and PAW-WPS incubated at 80 °C possessed considerably higher solubilities. This could be attributed to the high temperature of PAW damaging the double helical structure in amylopectin leading to more amylopectin leaching out and solubilizing (Y. Yan et al., 2020). In the case of the high amylose starches, we only observed a significant increase in the PAW starches incubated at 80 °C. The high temperature of the PAW could have facilitated the acid hydrolysis of the amorphous regions causing amylose to leach out and solubilize (Yan et al., 2020).

3.4. Water absorption capacity

There were no significant increases in the water absorption capacity (WAC) of the starches treated with PAW only compared to the control samples (Fig. 3) except for high amylose potato (97.5%). This exception suggests PAW induced a reorganization of the double helices in high amylose potato, and thereby enabled the starch to absorb more water. This phenomenon could be explained by the backbone model of amylopectin, which suggests flexibility for rearrangement of the double helices (Bertoft, 2017). Similarly, significant increases were observed in WPS (129.2%), and HAPS (114.2%) annealed with PAW, whereas the maize starches were unaffected. The WAC of all the starches incubated with PAW at 80 °C were significantly higher. At 80 °C, the starches were completely gelatinized and damaged (Jane et al., 1999). Thus, they had completely lost their granule structure and crystallinity and can absorb more water compared to the other starches (Tester and Morrison, 1990). Annealing of the starches with PAW also disrupts the crystalline sites and leads to the absorption of more water (Tester and Morrison, 1990; Pinkrová et al., 2011).

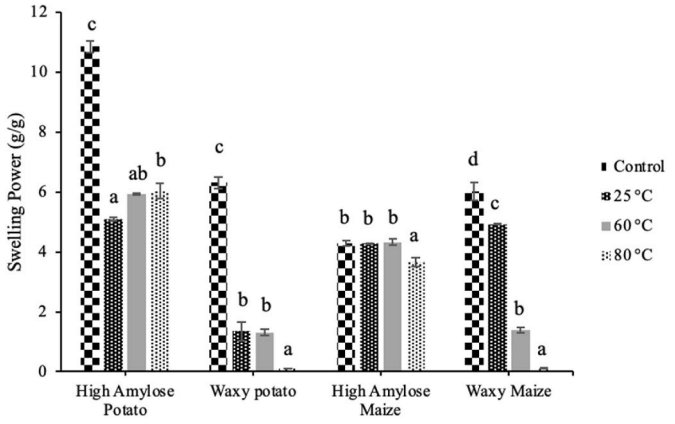

Fig. 1. Swelling power of PAW treated and untreated starches
Lowercase letters show significant differences ($p < 0.05$) between treated and untreated starches of the same type; Control = untreated starches, 25 °C = Plasma-activated water starch incubated at 25 °C, 60 °C = Plasma-activated water starch incubated at 60 °C, 80 °C = Plasma-activated water starch incubated at 80 °C.

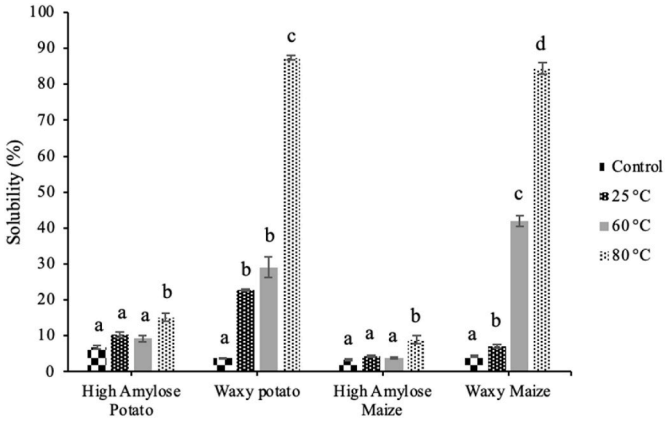

Fig. 2. Solubility of PAW treated and untreated starches
Lowercase letters show significant differences ($p < 0.05$) between treated and untreated starches of the same type; Control = untreated starches, 25 °C = Plasma-activated water starch incubated at 25 °C, 60 °C = Plasma-activated water starch incubated at 60 °C, 80 °C = Plasma-activated water starch incubated at 80 °C.

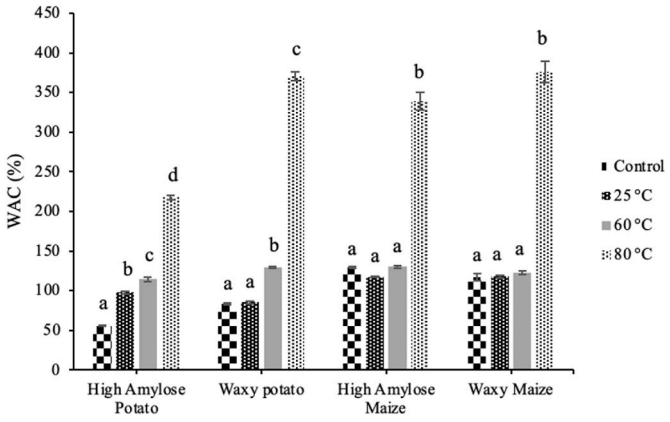

Fig. 3. Water Absorption Capacity of PAW treated and untreated starches
Lowercase letters show significant differences ($p < 0.05$) between treated and untreated starches of the same type; Control = untreated starches, 25 °C = Plasma-activated water starch incubated at 25 °C, 60 °C = Plasma-activated water starch incubated at 60 °C, 80 °C = Plasma-activated water starch incubated at 80 °C.

Correlations were performed to determine the relationships between the hydration properties of starches. Swelling power was negatively correlated with solubility ($r = -0.72$, $p = 0.002$), and water absorption capacity ($r = -0.56$, $p = 0.03$). Water absorption capacity was positively correlated with solubility ($r = 0.72$, $p = 0.002$). These correlations suggest that PAW treatment of starches at different temperatures enhanced the ability of these starches to hold water without necessarily swelling. On the other hand, starches modified with PAW at different temperatures would dissolve in solution relatively easily.

3.5. Fourier transform infrared spectroscopy-attenuated total reflectance (FTIR-ATR) measurement of treated and untreated starches

The infrared spectra of the treated and untreated starches are shown in Fig. 4. All the starches were characterized by bands at 765 cm^{-1} (C–C stretching), 860–866 cm^{-1} (C(1)-H, CH_2 deformation), 930–961 cm^{-1} (C–O–C skeletal mode of glycosidic linkage), 1018–1094 cm^{-1} (C–O–H bending), 1149–1162 cm^{-1} (C–O–C asymmetric stretching of the glycosidic bond), 1344–1348 cm^{-1} (C–O–H bending, CH_2 twisting), and 1415–1429 cm^{-1} (CH_2 bending, C–O–O stretch) (Kizil et al., 2002; Deeyai et al., 2013; Abdullah et al., 2018; Pozo et al., 2018). The band at 1640–1670 cm^{-1} shows the water adsorbed in the amorphous part of starch, while the bands at 2900-3000 cm^{-1} and 3000-3600 cm^{-1} correspond to the CH, CH_2 stretching region and O–H stretching region, respectively (Kizil et al., 2002; Deeyai et al., 2013; Abdullah et al., 2018; Pozo et al., 2018). The absorption bands of the treated and untreated starches were mostly overlapping. However, we observed a distinct reduction in peak height of the O–H stretching region compared to the controls in both potato starches (PAW-HAPS and PAW-WPS) treated at 80 °C and in PAW-HAMS at all temperatures. This suggests that treatments applied in this study did not induce the formation of any new hydroxyl functional groups in the starches (Thirumdas et al., 2017).

We also observed a slight increase in the peak height of the O–H stretching region in PAW-WMS 60 °C and PAW-WMS 80 °C, indicating the incorporation of new hydroxyl functional groups. We also observed distinct increases in the peak height of the C–OH bending region, CH_2 twisting region, CH_2 bending, C–O–O stretch, and CH, CH_2 stretching region in PAW-HAPS 80 °C. Although there was an elevation in the peak height of C–O–C skeletal mode of glycosidic linkage in PAW-HAPS 80 °C, this does not suggest the occurrence of cross-linking since there was no corresponding increase in the relative intensity (Table 3). However, treatment of starches with plasma-activated water induced the formation of cross-linking via ether linkages in PAW-WMS 80 °C and PAW-HAPS 25 °C (Zou et al., 2004; Okyere et al., 2019).

3.6. X-ray photoelectron spectroscopy analysis of treated and untreated starches

The major elements present in the starches were carbon and oxygen as shown by the XPS survey scan (Table 4). Minute quantities of nitrogen were detected in PAW-WMS 25 °C, PAW-WMS 60 °C, HAMS, PAW-HAMS 60 °C, HAPS, PAW-HAPS 25 °C, and PAW-HAPS 60 °C, which indicates the presence of protein residues on the starch granule surface (Russell et al., 1987; Saad et al., 2011). Also, it could be an indication of plasma-activated water inducing the formation of reactive nitrogen species on the granule surface in the case of PAW-WMS 25 °C and PAW-WMS 60 °C since we did not detect any nitrogen in the untreated WMS (Thirumdas et al., 2018). Trace quantities of silicon (Si_{2p}) was also detected on the surface of PAW-WMS 80 °C, PAW-WPS 60 °C, PAW-HAPS 25 °C, PAW-HAPS 60 °C, and PAW-HAPS 80 °C, which was due to contamination from the air (Russell et al., 1987; Saad et al., 2011). Starch has a theoretical O/C ratio of 0.83 based on the formula

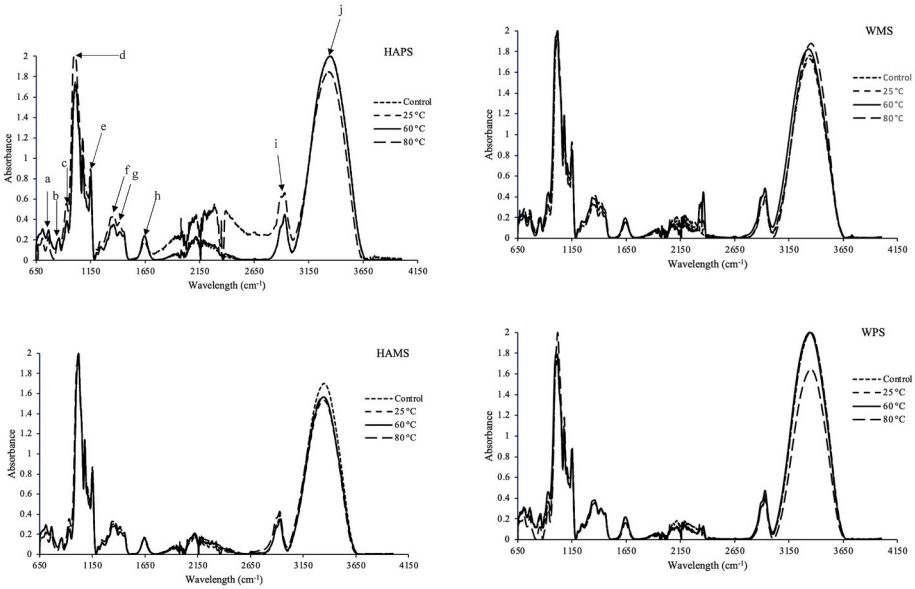

Fig. 4. FTIR-ATR spectra of PAW treated and untreated starches
HAPS = High Amylose Potato Starches, HAMS = High Amylose Maize Starches, WMS = Waxy Maize Starches and WPS = Waxy Potato starches. In all the graphs, Control = untreated Starches, 25 °C = Plasma-activated water starch incubated at 25 °C, 60 °C = Plasma-activated water starch incubated at 60 °C, 80 °C = Plasma-activated water starch incubated at 80 °C. a = C–C stretching, b = C (1)-H, CH_2 deformation, c = C–O–C skeletal mode of glycosidic linkage, d = C–O–H bending, e = C–O–C asymmetric stretching of the glycosidic bond, f = C–O–H bending, CH_2 twisting, g = CH_2 bending, C–O–O stretch, h = water adsorbed in the amorphous part of starch, i = CH, CH_2 stretching region, and j = O–H stretching region.

Table 3
Relative intensities of C–O–C glycosidic linkages after FTIR-ATR analysis.

Sample	Relative Intensities of C–O–C Glycosidic Linkages	
	930 cm^{-1}	1150 cm^{-1}
WMS	0.140	0.321
PAW-WMS 25 °C	0.137	0.305
PAW-WMS 60 °C	0.119	0.327
PAW-WMS 80 °C	0.141	0.343
HAMS	0.139	0.390
PAW-HAMS 25 °C	0.125	0.373
PAW-HAMS 60 °C	0.128	0.360
PAW-HAMS 80 °C	0.108	0.320
WPS	0.139	0.365
PAW-WPS 25 °C	0.137	0.337
PAW-WPS 60 °C	0.107	0.354
PAW-WPS 80 °C	0.151	0.348
HAPS	0.142	0.354
PAW-HAPS 25 °C	0.144	0.361
PAW-HAPS 60 °C	0.139	0.359
PAW-HAPS 80 °C	0.108	0.313

The different incubation temperatures for the starches are attached to the sample name.
WMS: Waxy Maize Starch, PAW-WMS 25 °C: Plasma-Activated Water Waxy Maize Starch 25 °C, PAW-WMS 60 °C: Plasma-Activated Water Waxy Maize Starch 60 °C, PAW-WMS 80 °C: Plasma-Activated Water Waxy Maize Starch 80 °C, HAMS: High Amylose Maize Starch, PAW-HAMS 25 °C: Plasma-Activated Water High Amylose Maize Starch 25 °C, PAW-HAMS 60 °C: Plasma-Activated Water High Amylose Maize Starch 60 °C, PAW-HAMS 80 °C: Plasma-Activated Water High Amylose Maize Starch 80 °C, WPS: Waxy Potato Starch, PAW-WPS 25 °C: Plasma-Activated Water Waxy Potato Starch 25 °C, PAW-WPS 60 °C: Plasma-Activated Water Waxy Potato Starch 60 °C, PAW-WPS 80 °C: Plasma-Activated Water Waxy Potato Starch 80 °C, HAPS: High Amylose Potato Starch, PAW-HAPS 25 °C: Plasma-Activated Water High Amylose Potato Starch 25 °C, PAW-HAPS 60 °C: Plasma-Activated Water High Amylose Potato Starch 60 °C, PAW-HAPS 80 °C: Plasma-Activated Water High Amylose Potato Starch 80 °C.

Table 4
Elemental surface composition (atomic %) and oxygen to carbon ratio of treated and untreated starches measured by XPS.

Samples	O_{1s} (%)	C_{1s} (%)	O_{1s}/C_{1s}	N_{1s} (%)	Si_{2p} (%)
WMS	45.5	54.5	0.83	–	–
PAW-WMS 25 °C	46.0	54.0	0.85	<0.1	–
PAW-WMS 60 °C	43.9	55.1	0.80	1.0	–
PAW-WMS 80 °C	46.7	52.5	0.89	–	0.8
HAMS	41.5	57.8	0.72	0.6	–
PAW-HAMS 25 °C	42.2	57.8	0.73	–	–
PAW-HAMS 60 °C	43.1	55.3	0.78	1.5	–
PAW-HAMS 80 °C	46.6	53.4	0.87	–	–
WPS	45.0	55.0	0.82	–	–
PAW-WPS 25 °C	44.5	55.5	0.80	–	–
PAW-WPS 60 °C	44.4	55.1	0.81	–	0.4
PAW-WPS 80 °C	45.2	54.8	0.82	–	–
HAPS	37.6	57.4	0.66	5.0	–
PAW-HAPS 25 °C	40.7	56.2	0.72	3.1	–
PAW-HAPS 60 °C	39.7	56.8	0.70	3.1	0.4
PAW-HAPS 80 °C	47.1	52.4	0.90	–	0.4

*The subscript on the elements denotes the orbital from which the electrons are displaced.
The different incubation temperatures for the starches are attached to the sample name.
WMS: Waxy Maize Starch, PAW-WMS 25 °C: Plasma-Activated Water Waxy Maize Starch 25 °C, PAW-WMS 60 °C: Plasma-Activated Water Waxy Maize Starch 60 °C, PAW-WMS 80 °C: Plasma-Activated Water Waxy Maize Starch 80 °C, HAMS: High Amylose Maize Starch, PAW-HAMS 25 °C: Plasma-Activated Water High Amylose Maize Starch 25 °C, PAW-HAMS 60 °C: Plasma-Activated Water High Amylose Maize Starch 60 °C, PAW-HAMS 80 °C: Plasma-Activated Water High Amylose Maize Starch 80 °C, WPS: Waxy Potato Starch, PAW-WPS 25 °C: Plasma-Activated Water Waxy Potato Starch 25 °C, PAW-WPS 60 °C: Plasma-Activated Water Waxy Potato Starch 60 °C, PAW-WPS 80 °C: Plasma-Activated Water Waxy Potato Starch 80 °C, HAPS: High Amylose Potato Starch, PAW-HAPS 25 °C: Plasma-Activated Water High Amylose Potato Starch 25 °C, PAW-HAPS 60 °C: Plasma-Activated Water High Amylose Potato Starch 60 °C, PAW-HAPS 80 °C: Plasma-Activated Water High Amylose Potato Starch 80 °C.

$(C_6H_{10}O_5)_n$ (Russell et al., 1987; Angellier et al., 2005). From our study, the experimental O/C ratio calculated using the sum of peak areas due to O–C–O (287.8) and C–O (286.5) as a measure of carbon content ranged from 0.66 to 0.90 in both treated and untreated starches. Except for WMS, all the experimental O/C ratio were either lower or higher than theoretical O/C ratio and thus indicates the presence of other surface components besides glucose polymers on the starch (Russell et al., 1987). These components could either be lipids or protein residues (Saad et al., 2011).

The C_{1s} core level spectrum was curve fitted to obtain four component peaks at 285 (C1), 286.5 (C2), 287.8 (C3), and 289.1 eV (C4) (Table 5). The peak at 285 eV is characteristic of a carbon bonded to a carbon and/or a hydrogen atom. The peak at 286.5eV denotes carbon singly bonded to an oxygen atom, while the peak at 287.8eV denotes carbon atoms bonded to two non-carbonyl oxygen atoms or to a single carbonyl oxygen atom. The final peak at 289.1eV is characteristic of carbon atoms bonded to a single oxygen atom and to a carbonyl oxygen (Russell et al., 1987; Angellier et al., 2005; Saad et al., 2011). The peaks observed at C–C/C–H and O–C═O further confirms the presence of lipids on the starch surface (Angellier et al., 2005; Wei et al., 2014). Plasma-activated water treatments of the starches successfully decreased the content of C1, C2 (except in PAW-HAMS 60 °C), while increasing the content of C4 in PAW-WMS 60 °C, PAW-WMS 80 °C, PAW-HAMS 60 °C and PAW-HAMS 80 °C. This indicates that these structures were disrupted during heat treatment and oxidized by the reactive species in PAW into carboxyl groups (Bie et al., 2016). Contrarily, we observed increases in the content of C1, C2, and C3 in PAW-WMS 25 °C (except C3), PAW-HAMS 25 °C (except C2 and C3), PAW-WPS 25 °C (except C2 and C3), PAW-WPS 60 °C (C2 and C3), PAW-WPS 80 °C (except C1), as well as PAW-HAPS 25 °C, 60 °C, and 80 °C, which suggests some level of polymerization taking place in these starches (Zhu, 2017). Overall, the XPS data show that PAW treatments of starches successfully altered the surface molecular structure of these starches.

4. Conclusion

Annealing the starches with plasma-activated water increases the gelatinization parameters and induces the formation of stable amylopectin crystals. Thus, these starches are stable during thermal treatment and can be used in canned foods. Plasma-activated water treatment at 80 °C is effective in increasing the water absorption capacity and solubility while decreasing the swelling power of the waxy and high amylose starches used in this study. FTIR-ATR data showed the occurrence of cross-linking in plasma-activated water waxy maize and high amylose potato starches incubated at 80 °C and 25 °C, respectively. Chemical surface analysis showed carbon and oxygen as the dominant elements in the starches, with some trace quantities of nitrogen and silicon. Plasma-activated water and incubation of the starches at ≥ 60 °C induced the oxidation of C–C/C–H and C–O in carboxyl groups. Overall, incubation of the starches at 60 °C and 80 °C during plasma-activated water treatment was more effective in altering the thermal and hydration properties, as well as the chemical surface of the starches. Starches modified with PAW at 60 °C and 80 °C can potentially be used as thickening agents. It is noteworthy to mention that although early research on starches has shown that treatment of starch at 60 °C and 80 °C in distilled water can alter starch properties, PAW is unique in that the presence of the reactive species and its acidic nature would enhance the modification of the starches to a much larger extent. However, further research would need to be conducted on the molecular weight, crystallinity, and rheology to understand the effect of PAW on starch

Table 5
Surface functional group composition obtained from curve fitting C1s XPS spectra of treated and untreated starches.

Samples	C1 (%)	C2 (%)	C3 (%)	C4 (%)
	C–C/C–H	C–O	O–C–O/ C═O	O–C═O-
Binding Energies (eV)	285.0 ± 0.3	286.5 ± 0.3	287.8 ± 0.3	289.1 ± 0.3
WMS	17.7	52.7	22.2	7.5
PAW-WMS 25 °C	19.1	56.5	19.7	4.7
PAW-WMS 60 °C	16.7	51.1	23.0	9.2
PAW-WMS 80 °C	7.9	31.3	41.5	19.3
HAMS	20.5	53.3	19.5	6.8
PAW-HAMS 25 °C	14.9	49.1	29.3	6.8
PAW-HAMS 60 °C	12.1	53.8	25.3	8.9
PAW-HAMS 80 °C	9.9	34.6	39.3	16.3
WPS	14.9	53.6	23.7	7.8
PAW-WPS 25 °C	17.8	53.3	22.5	6.4
PAW-WPS 60 °C	27.5	46.5	20.6	5.5
PAW-WPS 80 °C	12.1	56.5	27.2	4.3
HAPS	6.8	17.2	18.0	58.0
PAW-HAPS 25 °C	17.2	45.5	26.6	10.8
PAW-HAPS 60 °C	19.2	44.5	27.0	9.3
PAW-HAPS 80 °C	14.2	56.7	22.8	6.3

*The subscript on the elements denotes the orbital from which the electrons are displaced. The binding energy for the C_{1s} spectra is expressed as the mean ± standard deviation for each sample.
The different incubation temperatures for the starches are attached to the sample name.
WMS: Waxy Maize Starch, PAW-WMS 25 °C: Plasma-Activated Water Waxy Maize Starch 25 °C, PAW-WMS 60 °C: Plasma-Activated Water Waxy Maize Starch 60 °C, PAW-WMS 80 °C: Plasma-Activated Water Waxy Maize Starch 80 °C, HAMS: High Amylose Maize Starch, PAW-HAMS 25 °C: Plasma-Activated Water High Amylose Maize Starch 25 °C, PAW-HAMS 60 °C: Plasma-Activated Water High Amylose Maize Starch 60 °C, PAW-HAMS 80 °C: Plasma-Activated Water High Amylose Maize Starch 80 °C, WPS: Waxy Potato Starch, PAW-WPS 25 °C: Plasma-Activated Water Waxy Potato Starch 25 °C, PAW-WPS 60 °C: Plasma-Activated Water Waxy Potato Starch 60 °C, PAW-WPS 80 °C: Plasma-Activated Water Waxy Potato Starch 80 °C, HAPS: High Amylose Potato Starch, PAW-HAPS 25 °C: Plasma-Activated Water High Amylose Potato Starch 25 °C, PAW-HAPS 60 °C: Plasma-Activated Water High Amylose Potato Starch 60 °C, PAW-HAPS 80 °C: Plasma-Activated Water High Amylose Potato Starch 80 °C.

modification fully.

Funding

This research did not receive any specific grant from funding agencies in the public, commercial, or non-profit sectors.

CRediT authorship contribution statement

Akua Y. Okyere: Investigation, Writing – original draft, Conceptualization, Formal analysis, Methodology, Data curation. **Prince G. Boakye:** Writing – review & editing, Formal analysis, Methodology, Data curation. **Eric Bertoft:** Conceptualization, Formal analysis, Methodology, Data curation, Supervision, Resources, Writing – review & editing. **George A. Annor:** Conceptualization, Formal analysis, Methodology, Data curation, Supervision, Resources, Writing – review & editing.

Declaration of competing interest

The authors declare that they have no known competing financial interests or personal relationships that could have appeared to influence the work reported in this paper.

Acknowledgements

The authors are grateful to Professor Daniel D. Gallaher and Cynthia M. Gallaher (Department of Food Science and Nutrition, University of Minnesota) for their excellent assistance. Parts of this work was also carried out in the Characterization Facility, University of Minnesota, which receives partial support from NSF through the MRSEC program.

References

Aaliya, B., Sunooj, K.V., Navaf, M., Akhila, P.P., Sudheesh, C., Sabu, S., Sasidharan, A., Sinha, S.K., George, J., 2022. Influence of plasma-activated water on the morphological, functional, and digestibility characteristics of hydrothermally modified non-conventional talipot starch. Food Hydrocolloids 130, 107709. https://doi.org/10.1016/j.foodhyd.2022.107709.

Abdullah, A.H.D., Chalimah, S., Primadona, I., Hanantyo, M.H.G., 2018. Physical and chemical properties of corn, cassava, and potato starches. IOP Conf. Ser. Earth Environ. Sci. 160, 012003 https://doi.org/10.1088/1755-1315/160/1/012003.

Angellier, H., Molina-Boisseau, S., Belgacem, M.N., Dufresne, A., 2005. Surface chemical modification of waxy maize starch nanocrystals. Langmuir 21, 2425–2433. https://doi.org/10.1021/la047530j.

Annor, G.A., Marcone, M., Bertoft, E., Seetharaman, K., 2014. Physical and molecular characterization of millet starches. Cereal Chem. Journal 91, 286–292. https://doi.org/10.1094/CCHEM-08-13-0155-R.

Bemiller, J.N., 1997. Starch modification: challenges and prospects. Starch Staerke 49, 127–131. https://doi.org/10.1002/star.19970490402.

Bertoft, E., 2017. Understanding starch structure: recent progress. Agronomy 7, 56. https://doi.org/10.3390/agronomy7030056.

Bie, P., Pu, H., Zhang, B., Su, J., Chen, L., Li, X., 2016. Structural characteristics and rheological properties of plasma-treated starch. Innovat. Food Sci. Emerg. Technol. 34, 196–204.

Bogracheva, T.Ya, Wang, Y.L., Hedley, C.L., 2001. The effect of water content on the ordered/disordered structures in starches. Biopolymers 58, 247–259. https://doi.org/10.1002/1097-0282(200103)58:3<247::AID-BIP1002>3.0.CO;2-L.

Deeyai, P., Suphantharika, M., Wongsagonsup, R., Dangtip, S., 2013. Characterization of modified tapioca starch in atmospheric argon plasma under diverse humidity by FTIR spectroscopy. Chin. Phys. Lett. 30, 018103 https://doi.org/10.1088/0256-307X/30/1/018103.

Eliasson, A.-C., Ljunger, G., 1988. Interactions between amylopectin and lipid additives during retrogradation in a model system. J. Sci. Food Agric. 44, 353–361. https://doi.org/10.1002/jsfa.2740440408.

Han, X., Wen, H., Luo, Y., Yang, J., Xiao, W., Xie, J., 2022. Effects of chitosan modification, cross-linking, and oxidation on the structure, thermal stability, and adsorption properties of porous maize starch. Food Hydrocolloids 124, 107288. https://doi.org/10.1016/j.foodhyd.2021.107288.

Hizukuri, S., Kaneko, T., Takeda, Y., 1983. Measurement of the chain length of amylopectin and its relevance to the origin of crystalline polymorphism of starch granules. Biochim. Biophys. Acta Gen. Subj. 760, 188–191. https://doi.org/10.1016/0304-4165(83)90142-3.

Hizukuri, S., Takeda, Y., Yasuda, M., Suzuki, A., 1981. Multi-branched nature of amylose and the action of debranching enzymes. Carbohydr. Res. 94, 205–213. https://doi.org/10.1016/S0008-6215(00)80718-1.

Jane, J., Chen, Y.Y., Lee, L.F., McPherson, A.E., Wong, K.S., Radosavljevic, M., Kasemsuwan, T., 1999. Effects of amylopectin branch chain length and amylose content on the gelatinization and pasting properties of starch. Cereal Chem. Journal 76, 629–637. https://doi.org/10.1094/CCHEM.1999.76.5.629.

Kizil, R., Irudayaraj, J., Seetharaman, K., 2002. Characterization of irradiated starches by using FT-Raman and FTIR spectroscopy. J. Agric. Food Chem. 50, 3912–3918. https://doi.org/10.1021/jf011652p.

Laovachirasuwan, P., Peerapattana, J., Srijesdaruk, V., Chitropas, P., Otsuka, M., 2010. The physicochemical properties of a spray dried glutinous rice starch biopolymer. Colloids Surf. B Biointerfaces 78, 30–35. https://doi.org/10.1016/j.colsurfb.2010.02.004.

Li, H., Gidley, M.J., Dhital, S., 2019. High-amylose starches to bridge the "fiber gap": development, structure, and nutritional functionality: high-amylose starch to bridge "fiber gap". Compr. Rev. Food Sci. Food Saf. 18, 362–379. https://doi.org/10.1111/1541-4337.12416.

Lukes, P., Dolezalova, E., Sisrova, I., Clupek, M., 2014. Aqueous-phase chemistry and bactericidal effects from an air discharge plasma in contact with water: evidence for the formation of peroxynitrite through a pseudo-second-order post-discharge reaction of H_2O_2 and HNO_2. Plasma Sources Sci. Technol. 23, 015019 https://doi.org/10.1088/0963-0252/23/1/015019.

Lukes, P., Locke, B.R., Brisset, J.-L., 2012. Aqueous-Phase chemistry of electrical discharge plasma in water and in gas–liquid environments. In: Parvulescu, V.I., Magureanu, M., Lukes, P. (Eds.), Plasma Chemistry and Catalysis in Gases and Liquids. WILEY-VCH Verlag GmBH & Co. KGaA, Weinheim, Germany, pp. 243–308.

Matveev, Y.I., van Soest, J.J.G., Nieman, C., Wasserman, L.A., Protserov, V.A., Ezernitskaja, M., Yuryev, V.P., 2001. The relationship between thermodynamic and structural properties of low and high amylose maize starches. Carbohydr. Polym. 44, 151–160. https://doi.org/10.1016/S0144-8617(00)00211-3.

Noda, T., Isono, N., Krivandin, A.V., Shatalova, O.V., Błaszczak, W., Yuryev, V.P., 2009. Origin of defects in assembled supramolecular structures of sweet potato starches

with different amylopectin chain-length distribution. Carbohydr. Polym. 76, 400–409. https://doi.org/10.1016/j.carbpol.2008.10.029.
Oehmigen, K., Hähnel, M., Brandenburg, R., Wilke, Ch, Weltmann, K.-D., von Woedtke, Th, 2010. The role of acidification for antimicrobial activity of atmospheric pressure plasma in liquids: the role of acidification for antimicrobial. Plasma Process. Polym. 7, 250–257. https://doi.org/10.1002/ppap.200900077.
Okyere, A.Y., Bertoft, E., Annor, G.A., 2019. Modification of Cereal and Tuber Waxy Starches with Radio Frequency Cold Plasma and its Effects on Waxy Starch Properties. Carbohydr.
Perez, S., Bertoft, E., 2010. The molecular structures of starch components and their contribution to the architecture of starch granules: a comprehensive review. Starch Staerke 62, 389–420. https://doi.org/10.1002/star.201000013.
Pinkrova, J., Hubackova, B., Kadlec, P., Prihoda, J., Bubnik, Z., 2011. Changes of starch during microwave treatment of rice. Czech J. Food Sci. 21, 176–184. https://doi.org/10.17221/3496-CJFS.
Pozo, C., Rodríguez-Llamazares, S., Bouza, R., Barral, L., Castaño, J., Müller, N., Restrepo, I., 2018. Study of the structural order of native starch granules using combined FTIR and XRD analysis. J. Polym. Res. 25, 266. https://doi.org/10.1007/s10965-018-1651-y.
Pu, H., Chen, L., Li, X., Xie, F., Yu, L., Li, L., 2011. An oral colon-targeting controlled release system based on resistant starch acetate: synthetization, characterization, and preparation of film-coating pellets. J. Agric. Food Chem. 59, 5738–5745. https://doi.org/10.1021/jf2005468.
Qi, X., Tester, R.F., Snape, C.E., Ansell, R., 2003. Molecular basis of the gelatinisation and swelling characteristics of waxy rice starches grown in the same location during the same season. J. Cereal. Sci. 37, 363–376. https://doi.org/10.1006/jcrs.2002.0508.
Ratnayake, W.S., Hoover, R., Shahidi, F., Perera, C., Jane, J., 2001. Composition, molecular structure, and physicochemical properties of starches from four field pea (Pisum sativum L.) cultivars. Food Chem. 74, 189–202. https://doi.org/10.1016/S0308-8146(01)00124-8.
Russell, P.L., Gough, B.M., Greenwell, P., Fowler, A., Munro, H.S., 1987. A study by ESCA of the surface of native and chlorine-treated wheat starch granules: the effects of various surface treatments. J. Cereal. Sci. 5, 83–100. https://doi.org/10.1016/S0733-5210(87)80013-9.
Saad, M., Gaiani, C., Mullet, M., Scher, J., Cuq, B., 2011. X-Ray photoelectron spectroscopy for wheat powders: measurement of surface chemical composition. J. Agric. Food Chem. 59, 1527–1540. https://doi.org/10.1021/jf102315h.
Sarangapani, C., Ryan Keogh, D., Dunne, J., Bourke, P., Cullen, P.J., 2017. Characterisation of cold plasma treated beef and dairy lipids using spectroscopic and chromatographic methods. Food Chem. 235, 324–333. https://doi.org/10.1016/j.foodchem.2017.05.016.
Tester, R.F., Debon, S.J.J., 2000. Annealing of starch — a review. Int. J. Biol. Macromol. 27, 1–12. https://doi.org/10.1016/S0141-8130(99)00121-X.
Tester, R.F., Morrison, W.R., 1990. Swelling and gelatinization of cereal starches. I. Effects of amylopectin, amylose, and lipids. Cereal Chem. Journal 67, 551–557.
Thirumdas, R., Kadam, D., Annapure, U.S., 2017. Cold plasma: an alternative technology for the starch modification. Food Biophys. 12, 129–139. https://doi.org/10.1007/s11483-017-9468-5.
Thirumdas, R., Kothakota, A., Annapure, U., Siliveru, K., Blundell, R., Gatt, R., Valdramidis, V.P., 2018. Plasma activated water (PAW): chemistry, physico-chemical properties, applications in food and agriculture. Trends Food Sci. Technol. 77, 21–31. https://doi.org/10.1016/j.tifs.2018.05.007.
Vamadevan, V., Bertoft, E., Seetharaman, K., 2013. On the importance of organization of glucan chains on thermal properties of starch. Carbohydr. Polym. 92, 1653–1659. https://doi.org/10.1016/j.carbpol.2012.11.003.
Wei, B., Xu, X., Jin, Z., Tian, Y., 2014. Surface chemical compositions and dispersity of starch nanocrystals formed by sulfuric and hydrochloric acid hydrolysis. PLoS One 9, e86024. https://doi.org/10.1371/journal.pone.0086024.
Whistler, R.L., Bemiller, J.N., 2009. Starch: Chemistry and Technology, third ed. Academic Press.
Wu, X., Zhao, R., Wang, D., Bean, S.R., Seib, P.A., Tuinstra, M.R., Campbell, M., O'Brien, A., 2006. Effects of amylose, corn protein, and corn fiber contents on production of ethanol from starch-rich media. Cereal Chem. Journal 83, 569–575. https://doi.org/10.1094/CC-83-0569.
Yan, Y., Feng, L., Shi, M., Cui, C., Liu, Y., 2020. Effect of plasma-activated water on the structure and in vitro digestibility of waxy and normal maize starches during heat-moisture treatment. Food Chem. 306, 125589 https://doi.org/10.1016/j.foodchem.2019.125589.
Zhu, F., 2017. Plasma modification of starch. Food Chem. 232, 476–486. https://doi.org/10.1016/j.foodchem.2017.04.024.
Zou, J.-J., Liu, C.-J., Eliasson, B., 2004. Modification of starch by glow discharge plasma. Carbohydr. Polym. 55, 23–26. https://doi.org/10.1016/j.carbpol.2003.06.001.